
More Interpretable Graph Similarity Computation via Maximum Common Subgraph Inference

Zixun Lan^{1*} Binjie Hong^{2*} Ye Ma³ Fei Ma^{1†}

¹ Department of Applied Mathematics, School of Science

² Department of Information and Computing Science, School of Advanced Technology

³ Department of Financial and Actuarial Mathematics, School of Science
Xi'an Jiaotong-Liverpool University, SIP, 215123 Suzhou, China

{zixun.lan19, binjie.hong19}@student.xjtlu.edu.cn, {ye.ma, fei.ma}@xjtlu.edu.cn

Abstract

Graph similarity measurement, which computes the distance/similarity between two graphs, arises in various graph-related tasks. Recent learning-based methods lack interpretability, as they directly transform interaction information between two graphs into one hidden vector and then map it to similarity. To cope with this problem, this study proposes a more interpretable end-to-end paradigm for graph similarity learning, named Similarity Computation via Maximum Common Subgraph Inference (INFMCS). Our critical insight into INFMCS is the strong correlation between similarity score and Maximum Common Subgraph (MCS). We implicitly infer MCS to obtain the normalized MCS size, with the supervision information being only the similarity score during training. To capture more global information, we also stack some vanilla transformer encoder layers with graph convolution layers and propose a novel permutation-invariant node Positional Encoding. The entire model is quite simple yet effective. Comprehensive experiments demonstrate that INFMCS consistently outperforms state-of-the-art baselines for graph-graph classification and regression tasks. Ablation experiments verify the effectiveness of the proposed computation paradigm and other components. Also, visualization and statistics of results reveal the interpretability of INFMCS.

1 Introduction

Graph similarity measurement, which is to compute distance/similarity between two graphs, is a fundamental problem in graph-related tasks. It arises in a variety of real-world applications, such as graph search in graph-based database [43], malware detection [38], brain data analysis [24], etc. Graph Edit Distance (GED) [5] and Maximum Common Subgraph (MCS) [6] are two domain-agnostic graph similarity metrics, yet exact computation of both are known to be NP-hard [45]. For instance, no algorithm can compute the exact GED between graphs of more than 16 nodes within a reasonable time so far [3]. This problem has motivated interest in approximation algorithms, with a recent surge in graph similarity learning methods [19, 1, 2, 21, 46, 42, 18, 17].

Recent methods improve performance by capturing node-level or subgraph-level interactions. The initial way is to encode each graph as a graph-level fixed-length vector via Graph Neural Networks (GNNs) and then combine the two vectors of both input graphs to predict similarity. However, the actual difference between two graphs often arises from very small local substructures, resulting in

*Equal contribution

†corresponding author

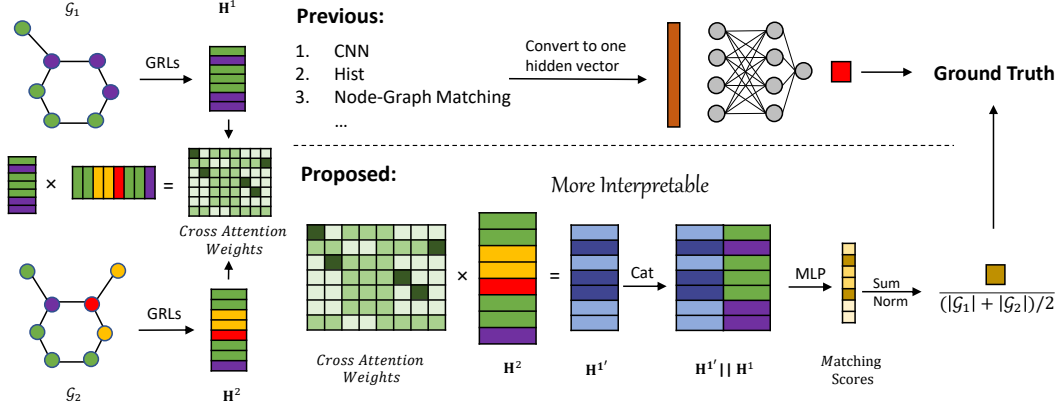


Figure 1: The entire flow of the proposed INFMCS framework. **(Previous:)** The previous method extracts hidden vectors from interactions of different scales and then maps them to the ground-truth similarity. It is less interpretable, and mapping hidden vectors to ground truth is also agnostic. **(Proposed:)** Our proposed model follows that the more similar a pair of graphs is, the greater the ratio of the MCS size to the pair’s average size is. Although only the ground-truth similarity score is used during training, we can infer the MCS from inside the model.

the graph-level fixed-length vector being difficult to contain local information [1]. To alleviate this problem, GMN [19], MGMN [21] and H2MN [46] derive node-level and graph-level embeddings containing interaction information of different scales through the cross-graph attention (propagation), and then convert these embeddings to one hidden vector (e.g. concatenation between two graph-level embeddings). SimGNN [1] and GraphSim [2] derive the corresponding hidden vector by applying the convolution operation to the pairwise node similarity matrix or extracting its histogram features respectively. Ultimately, all models map the hidden vector to the ground-truth similarity.

Previous methods lack interpretability despite the exploitation of interaction information. It is unclear what the final hidden vector represents and how to map it to ground truth. In natural language processing [35], it has been demonstrated that models with more interpretability tend to boost performance. Many tasks use attention, such as machine translation [23], language modelling [22], abstractive summarization [25]. Attention not only provides interpretability [40, 20, 10], but also benefits the performance of models. Without loss of generality, the graph similarity learning model with a more reasonable and interpretable paradigm can generally capture more critical information and filter out interference information, thus outperforming the less interpretable one.

To cope with this limitation, this study proposes a more interpretable end-to-end paradigm for graph similarity learning, named Similarity Computation via Maximum Common Subgraph Inference (INFMCS). Commonly, the more significant proportion of MCS to the average size of graph pairs [2], i.e. normalized MCS size (nMCS)³, the more similar the two graphs are. According to this fact, we infer Maximum Common Subgraph (MCS) implicitly and then obtain the normalized MCS size in an end-to-end fashion. First, we perform message passing from \mathcal{G}_2 to \mathcal{G}_1 by the modified cross-graph attention mechanism, thereby obtaining $|\mathcal{G}_1|$ pairs of node-level embeddings. In each pair, one embedding represents one node in \mathcal{G}_1 and the another embedding represents one node in \mathcal{G}_2 most likely matching the former. After concatenating the two embeddings in the embedding pair, we use MLP to transform the concatenation to the matching score between zero and one, where one and zero represent that two nodes are matched and not matched respectively. Finally, we add up the $|\mathcal{G}_1|$ matching scores as the predicted MCS size and then normalize it to derive the predicted similarity score. The entire process is optimized by either GED⁴/MCS normalized similarity or graph-graph classification label end-to-end. We also stack a few vanilla transformer encoder layers [36] with graph convolution layers to capture more global information, called Graph Convolution with Transformer (GCwT). Unlike the inherent order of sentences in natural language [36], graphs are permutation-invariant, resulting in no order for nodes. Thus we propose a novel Positional

³nMCS($\mathcal{G}_1, \mathcal{G}_2$) = $\frac{|\text{MCS}(\mathcal{G}_1, \mathcal{G}_2)|}{(|\mathcal{G}_1| + |\mathcal{G}_2|)/2}$. In this paper, we always view the graph with the smaller size as \mathcal{G}_1 , because the MCS size between two graphs is less than or equal to the size of the smaller graph.

⁴nGED($\mathcal{G}_1, \mathcal{G}_2$) = $\exp(\frac{-\text{GED}(\mathcal{G}_1, \mathcal{G}_2)}{(|\mathcal{G}_1| + |\mathcal{G}_2|)/2})$.

Encoding based on permutation-invariant node ordering. Comprehensive experiments demonstrate that INFMCS consistently outperforms state-of-the-art baselines for graph-graph classification and regression tasks. Ablation experiments verify the effectiveness of individual components, including the proposed graph similarity learning paradigm and GCwT with novel Positional Encoding. In brief, we highlight our main contributions as follows:

- We propose a more interpretable end-to-end paradigm for graph similarity learning. The interpretability is derived from inferring MCS implicitly.
- To our best knowledge, the proposed Positional Encoding based on permutation-invariant node ordering is the first being proposed and used in the graph-transformer related model for graph similarity task. Like the order of tokens in sentences, permutation-invariant node ordering is also an essential graph feature.
- We perform comprehensive experiments on six graph-graph regression datasets and two graph-graph classification datasets to verify the effectiveness of the INFMCS. Ablation experiments verify the effectiveness of individual components. Also, the case study and visualization demonstrate interpretability.

2 Related Work

Initial methods, such as SMPNN [29], GCNMEAN and GCNMAX [16] directly encode each graph as a graph-level fixed-length vector via GNNs and then only use graph-level interaction to predict similarity. After that, more models were proposed to exploit node-level or subgraph-level interactions by degrees. GMN [19] uses cross-graph attention to derive node-level embeddings that contain another graph’s information. SimGNN [1] and GraphSim [2] derive the corresponding hidden vector differently by applying the convolution operation to the pairwise node similarity matrix or extracting its histogram features. [42] first partitions graphs and then conducts node-wise comparison among subgraphs. MGMN [21] designs node-graph matching layers by comparing each node’s representation of one graph with the other whole graph representation. After converting graph to hypergraph via random walk or K-hop neighbourhood, H2MN [46] utilizes hypergraph convolution and subgraph matching blocks to predict similarity.

Compared with previous methods, our proposed INFMCS is simpler. INFMCS does not need to compute node-wise interactions per layer [19, 1] but only uses the last layer of node-level embeddings to capture cross-graph interactions. Second, ours does not need to consider multi-scale matching scores of $|\mathcal{G}_1| \times |\mathcal{G}_2|$ pairs [21], only calculates $|\mathcal{G}_1|$ matching scores. Third, ours does not need to preprocess graph data, such as graph partition [42] and hypergraph construction [46]. Although our method avoids the above computational burden, it achieves good performance.

3 Model Design

Our approach follows the hypothesis that the more similar a pair of graphs is, the greater the ratio of MCS size between graphs to the pair’s average size is. To achieve this, we first derive $|\mathcal{G}_1|$ pairs of node embeddings via cross-graph attention and then transform them into matching scores. Ideally, the sum of $|\mathcal{G}_1|$ matching scores is precisely equal to the size of MCS. Finally, we normalize the sum of these scores to predict the similarity. We also proposed a Graph Convolution with Transformer based on permutation-invariant Positional Encoding to fill a gap between the shallow GCN and the sizeable receptive field. The overall process is end-to-end and is outlined in Figure 1. Before describing the modules, we introduce relevant preliminaries that set the background for the remainder of the paper.

Graph Similarity Learning Given a pair of input graphs $(\mathcal{G}_1, \mathcal{G}_2)$, the aim of graph similarity learning is to produce a similarity score $y = s(\mathcal{G}_1, \mathcal{G}_2) \in \mathcal{Y}$. The graph $\mathcal{G}_1 = (\mathcal{V}_1, \mathcal{E}_1)$ is represented as a set of N nodes $v_i \in \mathcal{V}_1$ with a feature matrix $X_1 \in \mathcal{R}^{N \times d}$, edges $(v_i, v_{i'}) \in \mathcal{E}_1$ formulating an adjacency matrix $A_1 \in \mathcal{R}^{N \times N}$. Similarly, the second graph $\mathcal{G}_2 = (\mathcal{V}_2, \mathcal{E}_2)$ can be represented in the same way. For graph-graph classification task, the scalar y represents the class label, i.e., $y \in \mathcal{Y} = \{0, 1\}$; for graph-graph regression task, the scalar y measures the graph similarity, i.e., $y \in \mathcal{Y} = [0, 1]$.

3.1 Similarity Computation

Notably, we always view the graph with the smaller size as \mathcal{G}_1 , since the MCS size between two graphs is less than or equal to the size of the smaller graph in this paper. Given the node representations of the last layer of the graph representation learning $\mathbf{H}^1 = [\mathbf{h}_1^1; \mathbf{h}_2^1; \dots; \mathbf{h}_{|\mathcal{V}_1|}^1] \in \mathcal{R}^{|\mathcal{V}_1| \times d}$ for \mathcal{G}_1 and $\mathbf{H}^2 = [\mathbf{h}_1^2; \mathbf{h}_2^2; \dots; \mathbf{h}_{|\mathcal{V}_2|}^2] \in \mathcal{R}^{|\mathcal{V}_2| \times d}$ for \mathcal{G}_2 , we pass the message from \mathcal{G}_2 to \mathcal{G}_1 by modified cross-graph attention a_{ij} , and then obtain the representation $\mathbf{h}_{i'}^1 \in \mathcal{R}^{1 \times d}$ of node $v_j \in \mathcal{V}_2$ that most likely matches node $v_i \in \mathcal{V}_1$:

$$a_{ij} = \frac{\exp(s_h(\mathbf{h}_i^1, \mathbf{h}_j^1) \times \tau_*^{-1})}{\sum_{j'} \exp(s_h(\mathbf{h}_i^1, \mathbf{h}_{j'}^1) \times \tau_*^{-1})}, \mathbf{h}_{i'}^1 = \sum_j a_{ij} \mathbf{h}_j^1, \quad (1)$$

where s_h is a vector space similarity metric, like Euclidean or cosine similarity. In order to discretize a_{ij} , we add a learnable parameter $\tau_* \in (0, 1]$. In other words, it makes the weight a_{ij} of one node $v_j \in \mathcal{V}_2$ ($j = \operatorname{argmax}_{j'} a_{ij'}$) tend to one and the others tend to zero due to $\sum_{j'} a_{ij'} = 1$. Thus, $\mathbf{h}_{i'}^1$ represents the representation of node corresponding to node v_i with the highest probability.

After concatenating \mathbf{h}_i^1 with $\mathbf{h}_{i'}^1$, we transform the concatenation to the matching score s_i by MLP. Ideally, the sum of $|\mathcal{G}_1|$ matching scores is precisely equal to the size of MCS. Finally, we normalize the sum of these predicted scores to compute similarity \hat{y}_i :

$$\hat{y} = \frac{\sum_i s_i}{(|\mathcal{G}_1| + |\mathcal{G}_2|)/2}, s_i = \operatorname{sigmoid}(\operatorname{MLP}(\mathbf{h}_i^1 \parallel \mathbf{h}_{i'}^1)). \quad (2)$$

The loss functions are defined as follows:

$$\mathcal{L}_c = -\frac{1}{|\mathcal{D}|} \sum_{i=1}^{|\mathcal{D}|} y_i \log(\hat{y}_i) + (1 - y_i) \log(1 - \hat{y}_i) \text{ or } \mathcal{L}_r = \frac{1}{|\mathcal{D}|} \sum_{i=1}^{|\mathcal{D}|} (y_i - \hat{y}_i)^2, \quad (3)$$

where \mathcal{L}_c represents the binary cross-entropy loss for the graph-graph classification task and \mathcal{L}_r is the mean square error loss for the graph-graph regression task. y_i denotes the ground-truth supervision information, and $|\mathcal{D}|$ is the size of the dataset.

3.2 Graph Convolution with Transformer

Before exploiting node-wise interactions, we need to obtain node-level embeddings as in the previous method. GCN [15] is the most popular spatial graph convolution. In this study, we use it to compute node-level embeddings. For simplicity, we denote the encoding process by $\operatorname{GCN}(\cdot)$ and describe architectural details in the appendix. The GCN computes node representations $\mathbb{H} \in \mathcal{R}^{|\mathcal{V}| \times d}$ via

$$\mathbb{H} = [\mathbf{h}_1; \mathbf{h}_2; \dots; \mathbf{h}_{|\mathcal{V}|}], \mathbf{h}_i = \operatorname{GCN}(\mathcal{G}, \mathbf{x}_i, \{\mathbf{x}_{ij}\}_{j \in \mathcal{N}(i)}), \quad (4)$$

where $\mathbf{h}_i \in \mathcal{R}^{1 \times d}$ and $\mathcal{N}(i)$ denotes the node representation and neighbors of node v_i respectively. Graph similarity learning requires not only node embeddings to perceive local information but also node representations to contain global information due to many subtle differences across the whole graph [2, 46]. However, over-smoothing [33, 15] constrains graph convolution from stacking multiple layers, resulting in a gap between the shallow GCN and the sizeable receptive field.

To fill this gap, we stack some vanilla transformer encoder layers [36] with graph convolution layers to capture more global information naturally. The global perception ability of Transformer comes from the self-attention mechanism, which internally calculates the correlation between embeddings. The attention weight matrix is equivalent to constructing a fully connected graph, and then message passing is based on this fully connected structure. For sentence representation [36], extensive experiments show the importance of Positional Encoding. Sentences with the same tokens but in different order have different semantics (Figure 2), which shows that order is also an inherent feature of sentences. However, graphs are permutation-invariant, resulting in no order for nodes. Thus, we propose a permutation-invariant node ordering $\mathbf{C} \in \mathcal{R}^{|\mathcal{V}|}$ based on closeness centrality [41]:

$$\mathbf{C} = \operatorname{argtop}_{|\mathcal{V}|}([c_1, c_2, \dots, c_{|\mathcal{V}|}]), c_i = \frac{n-1}{|\mathcal{V}|-1} \frac{n-1}{\sum_{j=1}^{n-1} d(j, i)}, \quad (5)$$

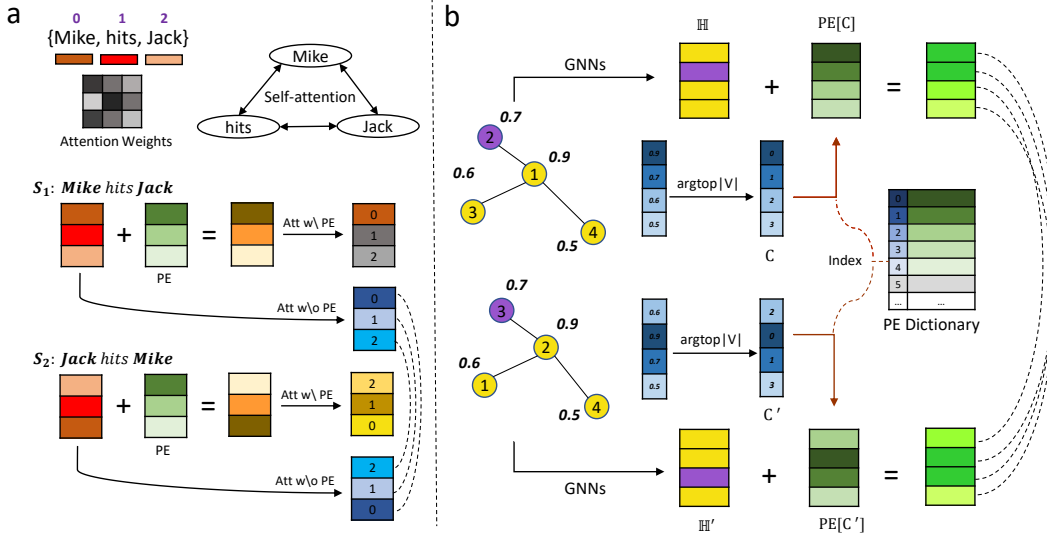


Figure 2: **a**: Sentences with the same tokens but in different order have different semantics, which shows that order is also an inherent feature of sentences. For example, sentence s_1 and sentence s_2 have different semantics, while the same token gets the identical representation by directly using self-attention without PE. **b**: Our proposed Positional Encoding is permutation-invariant. Even if the nodes in the graph are re-permuted, the Positional index for these nodes does not change.

where c_i is the closeness centrality of node v_i . It is the reciprocal of the average shortest path distance to v_i over all other nodes, and higher closeness values indicate higher centrality. Besides, n is the number of nodes in the connected part of the graph containing the node v_i and $\frac{n-1}{|\mathcal{V}|-1}$ is the proportion of this connected component in the entire graph. Hence, Eq. 5 can be generalized to graphs with more than one connected component, where the size of the connected component scales each node. $\text{argtop}|\mathcal{V}|(\cdot)$ calculates the rank of each element in the vector in descending order. For example, $\text{argtop}|\mathcal{V}|([0.4, 0.6, 0.1, 0.9]) = [2, 1, 3, 0]$. Our model also generalizes to edge representations. We convert the original graph to a line graph and then compute the permutation-invariant node order since the edges in the original graph construct the nodes in the line graph.

We denote the vanilla transformer encoder by $\text{TransformerEncoder}(\cdot)$ for simplicity and describe architectural details in appendix. Given a learnable Positional Encoding dictionary $\mathbf{PE} \in \mathcal{R}^{m \times d}$ ($m \gg |\mathcal{V}|$), final node representations $\mathbf{H} \in \mathcal{R}^{|\mathcal{V}| \times d}$ is derived by Eq. 6:

$$\mathbf{H} = \text{TransformerEncoder}(\mathcal{H}), \mathcal{H} = \mathbb{H} + \mathbf{PE}[\mathbf{C}], \quad (6)$$

where $\mathbf{PE}[\mathbf{C}] \in \mathcal{R}^{|\mathcal{V}| \times d}$ is Positional Encoding according to the node ordering \mathbf{C} .

4 Evaluation

In this section, we systematically evaluate the performance of our INFMCS with comparison to recently proposed state-of-the-art approaches for both the graph-graph classification and graph-graph regression tasks, and with significant goals of addressing the following questions: **Q1**: How effective, efficient and robust is INFMCS compared to the state-of-the-art approaches under MCS/GED metric? **Q2**: How does the proposed similarity computation paradigm and GCwT with permutation-invariant Positional Encoding improve performance? **Q3**: Does INFMCS have stronger interpretability?

Data For graph-graph classification task, we use **FFmpeg**⁵ and **OpenSSL**⁶ [21] as datasets, where each graph denotes binary function's control flow graph (CFG). Therefore, we take two CFGs compiled from the same source code as positive samples, i.e., $s(\mathcal{G}_1, \mathcal{G}_2) = 1$, and the dissimilar CFGs compiled from different source code, i.e., $s(\mathcal{G}_1, \mathcal{G}_2) = 0$. Moreover, we split each dataset

⁵<https://ffmpeg.org/>

⁶<https://www.openssl.org/>

Table 1: Graph-Graph classification results (AUC score) with standard deviation (in percentage).

Datasets	FFmpeg			OpenSSL		
	[3, 200]	[20, 200]	[50, 200]	[3, 200]	[20, 200]	[50, 200]
SimGNN	95.38±0.76	94.32±1.01	93.45±0.54	95.96±0.31	93.38±0.82	94.25±0.85
GMN	94.15±0.62	95.92±1.38	94.76±0.45	96.43±0.61	93.03±3.81	93.91±1.65
GraphSim	97.46±0.30	96.49±0.28	94.48±0.73	96.84±0.54	94.97±0.98	93.66±1.84
MGMN	98.07±0.06	98.29±0.10	97.83±0.11	96.90±0.10	97.31±1.07	95.87±0.88
PSimGNN	96.67±0.54	96.86±0.95	95.23±0.15	96.10±0.46	94.67±1.30	93.46±1.59
GOTSim	96.93±0.34	97.01±0.52	95.65±0.31	97.87±0.49	96.42±1.89	95.97±1.06
H2MN	98.28±0.20	98.54±0.14	98.30±0.29	98.27±0.16	98.47±0.38	97.78±0.75
INFMCS	98.49±0.09	99.36±0.13	99.48±0.20	98.34±0.20	99.14±0.31	99.26±0.45

into 3 sub-datasets according to the graph size in order to investigate the impact of graph size. For graph-graph regression task, we employ three real datasets and three sythetic datasets, including **AIDS(2-15)**, **LINUX(2-15)**, **PTC_MM(all)**, **BA100**, **BA200** and **BA300**. We extract graphs from the original datasets (**AIDS** [30], **LINUX** [39], **PTC_MM** [11])⁷ and construct the above three real datasets, where the values in parentheses indicate the size range of extracted graph. To verify the performance on large graphs, we also use the Barabási–Albert model [13] to generate sythetic graphs. We generated three sythetic datasets with graph sizes around 100, 200, and 300 respectively, called **BA100**, **BA200** and **BA300**. Detailed descriptions and statistics of both real and sythetic datasets can be found in the appendix.

Evaluation For the graph-graph classification task, we use *Area Under the Curve (AUC)* [4] to evaluate the model. For the graph-graph regression task, we use *averaged Mean Squared Error (mse)*, *Spearman’s Rank Correlation Coefficient (ρ)* [34] and *Precision at k ($p@k$)* to test the accuracy and ranking performance. To avoid information leakage, we let the model compute the similarity between the query graph and each graph in the original test set to rank.

Baselines We use eight SOTA learning-based methods as baselines, including GMN [19], SimGNN [1], GraphSim [2], MGMN [21], H2MN [46], GOTSim [7], PSimGNN [42], EMBAVG [2] and SMPNN [29]. Besides methods PSimGNN [42] and EMBAVG [2], we use the source code released by the authors for the regression task. We reproduced the above two baselines according to the original papers. We also tune their hyperparameters on the validation set on the regression task. For the classification task, we use the AUC scores reported in [46] as the results for each baseline. We also use five classical algorithms as baselines to compare running time, including A* [32], MCSPLIT [26], BEAM [27], HUNGARIAN [31], VJ [8] and HED [9].

Implementation Settings Our proposed INFMCS is implemented with Deep Graph Library (DGL) [37] and Pytorch [28]. Regarding the model’s hyperparameters, we fix the number of GCN layers to 3. We search the number of Transformer layers $L \in \{2, 4, 6, 8\}$ and the dimension of hidden layers $d \in \{128, 256, 512\}$, where the dimension of all hidden layers is set to the same. More details about the hyper-parameter search can be found in the appendix. We conduct all the experiments on a machine with an Intel Xeon 4114 CPU and two Nvidia Titan GPU. As for training, we use the Adam algorithm for optimization [14] and fix the initial learning rate to 0.001. The proposed model is trained on real datasets for 100 epochs with a batch size of 128 and on sythetic datasets for 30 epochs with a batch size of 32. Checkpoints are saved for each epoch to select the best checkpoints on the evaluation set. The source code can be found in the supplementary materials.

4.1 Overall Performance

Graph-Graph Classification Task We operate the training process five times and report the mean and standard deviation in *AUC*. Our method is straightforward and achieves state-of-the-art performance on both datasets under all settings. The graph-graph classification performance is illustrated in Table 1. We have two observations. **First**, compared with GMN [19], SimGNN [1] and GraphSim [2], our method obtains relative gains around 5%. It indicates that our method makes better use of node-wise interactions. **Second**, compared with PSimGNN [42] and H2MN [46], our method obtains relative gains of around 2%. It implies that the improvement of graph representation ability can

⁷<https://chrsmrrs.github.io/datasets/docs/datasets/>

Table 2: Graph-Graph regression results about $\text{mse}(\times 10^{-2})$, ρ and $\text{p}@10$ on the MCS metric.

Datasets	AIDS(2-15)			LINUX(2-15)			PTC_MM(all)		
	mse↓	ρ ↑	$\text{p}@10$ ↑	mse↓	ρ ↑	$\text{p}@10$ ↑	mse↓	ρ ↑	$\text{p}@10$ ↑
EMBAVG	33.20	0.0045	0.0540	0.83	0.5922	0.1340	35.03	0.0497	0.3471
GMN	32.20	0.0039	0.0578	3.99	0.0561	0.1340	35.03	0.0370	0.3500
GraphSim	2.73	0.1688	0.0578	0.81	0.2260	0.1340	3.21	0.5001	0.3500
SimGNN	2.65	0.1784	0.0596	0.83	0.4281	0.2370	3.27	0.5280	0.3500
SMPNN	2.89	0.2046	0.1056	12.59	0.5502	0.4280	4.67	0.4558	0.4353
MGMN	1.69	0.5300	0.1683	0.87	0.5351	0.3664	1.43	0.7329	0.5200
PSimGNN	2.54	0.1031	0.0452	1.83	0.4311	0.2668	3.43	0.4359	0.4280
GOTSim	1.77	0.5550	0.1763	0.61	0.3752	0.2569	2.75	0.3495	0.3431
H2MN	1.29	0.6745	0.2097	0.44	0.6364	0.4795	1.07	0.8823	0.7182
INFMCS	0.30	0.9352	0.7976	0.02	0.9814	0.8870	0.71	0.9205	0.7794

Table 3: Graph-Graph regression results about $\text{mse}(\times 10^{-2})$ on the synthetic datasets.

Datasets	BA100		BA200		BA300	
	mse(MCS)	mse(GED)	mse(MCS)	mse(GED)	mse(MCS)	mse(GED)
EMBAVG	16.21	10.581	20.24	9.171	21.79	12.732
GMN	16.21	8.831	20.24	9.002	20.14	8.756
GraphSim	0.20	0.065	0.44	0.140	0.57	0.062
SimGNN	0.20	0.060	0.05	0.180	0.02	0.110
SMPNN	1.10	22.530	0.32	23.920	0.24	24.290
MGMN	0.35	1.033	0.27	0.901	0.44	0.071
PSimGNN	0.48	1.932	0.51	1.366	0.67	0.103
H2MN	0.02	0.187	0.01	0.532	0.02	0.034
INFMCS	5.49e-7	0.061	1.80e-5	0.011	0.003	0.005

benefit experimental results. A more detailed analysis can be found in the ablation study. **Notably**, we only exploit node-wise interactions at the last layer, while the previous method exploits the interaction information at each layer. It shows that our computational paradigm is simpler and has less complexity. Moreover, the construction process of the classification label is inconsistent with the internal logic of our method. It demonstrates that our method is robust even if the labels are MCS-independent.

Graph-Graph Regression Task For the graph-graph regression task, we also conduct the experiments five times and report their mean performance. The detailed performances on real and synthetic datasets are demonstrated in Table 2 and 3. The results for the GED metric can be found in the appendix. Our model achieves state-of-the-art performance on both MCS and GED metrics. In general, we can obtain similar conclusions as to the classification task. As for synthetic datasets, we observe that our method still outperforms other methods. It shows that our method can be adapted to bigger graphs. Notably, the results of our method on the MCS metric are about eight times better than those on the GED metric. We infer that this situation results from the model’s internal logic consistent with the MCS label. The MSE of the model prediction results is close to zero, which means we can infer a more accurate MCS based on the average size of the input graph pairs. It increases the interpretability.

Efficiency We show the running time between different methods in Figure 4 in order to evaluate the efficiency of INFMCS. As we can see, the learning-based approaches are consistently faster than the traditional methods in all datasets, especially the exact algorithm MCSPLIT. We also observe that INFMCS is faster than other learning-based approaches. We attribute the efficiency gains to two points. First, unlike previous methods that exploit the interaction information of each layer, our method only needs to compute the interaction information of the last layer. Second, our method does not require building hypergraphs or graph partitions.

Hyperparameter sensitivity analysis We fixed the number of Transformer layers L to 8 and the dimension of hidden layers d to 256 to explore the impact of several vital hyper-parameters on OpenSSL subsets (Figure 5). The performance under different hyperparameters is consistent, revealing the robustness of our method. We observe that the performance of INFMCS improves as the number

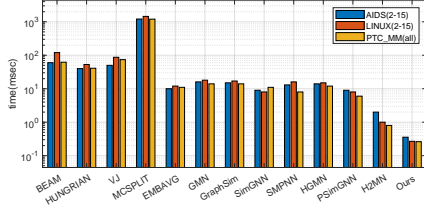


Figure 4: Running time comparisons.

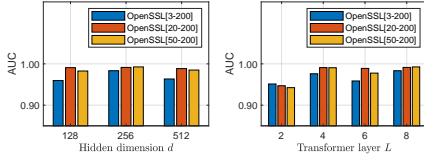


Figure 5: Sensitive analysis of test set.

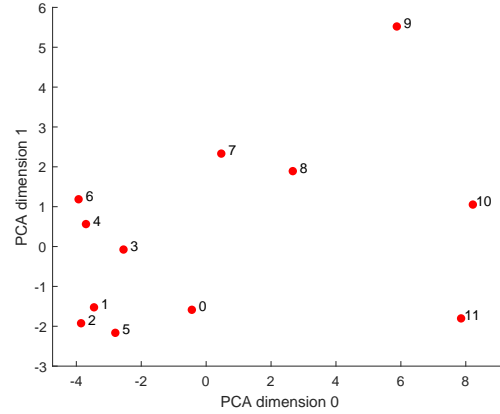


Figure 6: Positional Encoding analysis.

of Transformer layers increases. We hypothesise that more Transformer layers allow node-level embeddings to contain more global information, thus improving experimental results. A comparison of the number of parameters of our method with other baselines can be found in appendix.

4.2 Ablation Study

BASE⁸ denotes the proposed similarity computation paradigm whose graph representation model (GRM) is GCN. **BASE+T**'s GRM is GCwT without the permutation-invariant Positional Encoding. **BASE+T+PE**'s GRM is GCwT with the permutation-invariant Positional Encoding. **BASE+H_{rw}**'s GRM is hypergraph convolution used in [46]. We use the part of their code⁹ to obtain node embeddings and then pass these to our paradigm end-to-end¹⁰. **H2MN-H** denotes that the H2MN model's hyperparameter k is set to 1, indicating that hypergraph convolution degenerates to GCN. The results of the ablation study is illustrated in Table 4 and 5, and on which we have the four observations: **1) BASE** outperforms previous methods except for H2MN, thus we compare **BASE** with **H2MN-H** in order to demonstrate the effectiveness of the computation paradigm. We find **BASE** outperforms **H2MN-H**, which means more interpretable forward computation can improve performance. **2) BASE+T** has lower performance than **BASE**. It indicates that the performance of GCwT without the permutation-invariant Positional Encoding degrades. We attribute the reason to the loss of graph structural information since stacking Transformer layers only is equivalent to treating the graph as a fully connected graph. **3) BASE+T+PE** outperforms **BASE**, which confirms that GCwT with the permutation-invariant Positional Encoding not only increases the receptive field of the node but also learns the structural information through PE. More on Positional Encoding analysis can be found in the next subsection. **4) BASE+T+PE** outperforms **BASE+H_{rw}**, implying that GCwT can be better adapted to the proposed computation paradigm and have decent global representation.

Table 4: Ablation study on the FFmpeg.

(AUC score)	3-200	20-200	50-200
H2MN-H	97.50	98.12	98.05
BASE	98.16	98.83	98.87
BASE+T	97.13	98.20	98.48
BASE+H	98.01	98.42	98.56
BASE+T+PE	98.49	99.36	99.49

Table 5: Ablation study on the MCS metric.

(mse $\times 10^{-2}$)	AIDS	LINUX	PTC_MM
H2MN-H	1.63	0.56	1.18
BASE	1.41	0.36	0.98
BASE+T	3.21	0.93	1.24
BASE+H	1.70	0.21	1.02
BASE+T+PE	0.30	0.02	0.71

⁸MCS-RSC is MCS-Related Similarity Computation. BASE = GCN + MCS-RSC; BASE+T = GCwT-w/o-PE + MCS-RSC; BASE+T+PE = GCwT-w/-PE + MCS-RSC; BASE+H = HyperGCN + MCS-RSC; H2MN-H = GCN + H2MN-RSC.

⁹<https://github.com/cszhangzhen/H2MN>

¹⁰We use the random walk to construct the hypergraph and set hyperparameter k to 5

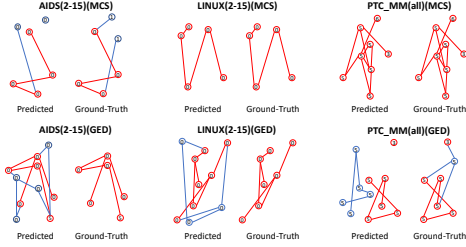


Figure 6: Visualizations of inferring MCS.

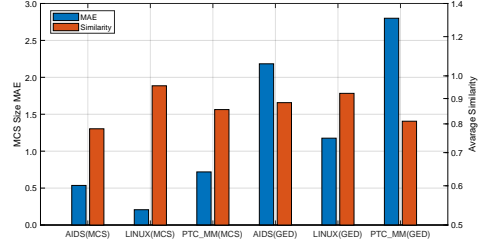


Figure 7: Interpretability analysis.

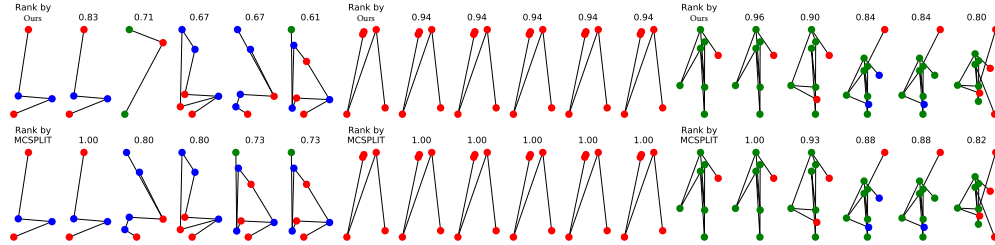


Figure 8: Visualization of ranking results. From left to right: AIDS, LINUX, PTC_MM.

4.3 Inteptrability Analysis, Case Study and Discussion

Positional Encoding We reduce the Positional Encoding trained on AIDS(2-15) to two dimensions via PCA and present them in Fig. 6, where each red point denotes a Positional Encoding. Since the size of most samples is no more than 12, embeddings after position 12 are insufficiently trained. We present the top 12 Positional Encoding embeddings and obtain an exciting observation. The Euclidean distance between Positional Encoding 0 and the following Positional Encoding gradually increases. The Euclidean distance here corresponds to each node’s centrality in the graph, which means the Positional Encoding embeddings preserve the graph’s structural information well.

Infer MCS During inference, we infer the MCS size m via multiplying the average size of the graph pair by the similarity score. Next, we extract a subgraph from \mathcal{G}_1 that consists of nodes corresponding to the top m matching scores s in Eq. 2. Also, we use MCSPLIT to extract the true MCS. To evaluate the quality of our predicted MCS, we compute the similarity between the predicted and the actual MCS. The similarity results and some visualizations are presented in Fig. 6 and 7, where red subgraphs are MCS between the predicted and the actual MCS. The mean absolute error between the predicted and actual sizes is larger on the GED metric. We attribute the reason to the inconsistency in the model logic and the label construction process. However, we note that the similarity between the predicted MCS and the ground-truth MCS is higher than 0.8 on both metrics except for the AIDS (MCS) results, revealing the interpretability of our approach. We can predict the similarity score and infer MCS to understand why this similarity score is predicted.

Case Study We demonstrate three example queries, one from each dataset in Fig. 8. The first row shows the graphs returned by our model in each demo, with the predicted similarity for each graph shown at the top. The bottom row describes the graphs returned by MCSPLIT. Notably, the top 5 results are precisely the isomorphic graphs to the query in the case of LINUX and PTM_MM.

Why is INFMCS effective? For the computation paradigm, our method ultimately only needs to consider n pairs of interaction information, which means it captures more critical information that affects the similarity compared to previous methods. Since Positional Encoding well preserves the positional information of nodes, the interaction within the model compares the similarity of local structures between nodes and considers the relative position between nodes in two graphs. Intuitively, the more similar the two graphs are, the more similar their corresponding local regions should be.

5 Conclusion

This paper proposes a more interpretable end-to-end paradigm for graph similarity learning, whose interpretable computation process improves the performance of graph similarity learning. The model can implicitly infer Maximum Common Subgraph during inference. We stack some vanilla transformer encoder layers with graph convolution layers and propose a novel permutation-invariant node Positional Encoding to capture more global information. Comprehensive experiments and ablation studies demonstrate that INFMCS outperforms previous methods and is more interpretable.

A Graph Convolution Layer

We describe the computation process of one layer in $\text{GCN}(\cdot)$:

$$u_i^{n+1} = \text{ReLU} \left(\sum_{j \in \mathcal{N}(i)} \frac{1}{\sqrt{d_i d_j}} u_j^n \mathbf{W}^{(n)} + b^{(n)} \right). \quad (7)$$

Here, $u_i^{(n)} \in \mathbb{R}^{D^{(n)}}$ and $u_i^{(n+1)} \in \mathbb{R}^{D^{(n+1)}}$ are representations of node i at n -th and $n + 1$ -th layer. $\mathcal{N}(i)$ is the set of the first-order neighbors of node i plus i itself. d_i is the degree of node i plus 1. $\mathbf{W}^{(n)} \in \mathbb{R}^{D^{(n)} \times D^{(n+1)}}$ is the weight matrix of the n -th GCN layer. $b^{(n)} \in \mathbb{R}^{D^{(n+1)}}$ is the bias, $D^{(n)}$ denotes the dimension of embedding vector at layer n . $\text{ReLU}(x) = \max(0, x)$ is the activation function.

B Transformer Encoder Layer

Each Transformer Encoder Layer has two parts: a self-attention module and a position-wise feed-forward network (FFN):

$$Q^h = H^{(l)} W_Q^h, \quad K^h = H^{(l)} W_K^h, \quad V^h = H^{(l)} W_V^h, \quad (8)$$

$$A^h = \frac{Q^h K^{h\top}}{\sqrt{d_K}}, \quad H^h = \text{softmax}(A^h) V^h, \quad (9)$$

$$H' = W \cdot (\|_h H^h) + H^{(l)} \quad (10)$$

$$H^{(l+1)} = \text{FFN}(\text{LN}(H')) + H'. \quad (11)$$

Here, $H^{(l)} = \left[h_1^{(l)\top}, \dots, h_n^{(l)\top} \right]^\top \in \mathbb{R}^{n \times d}$ denote the input of self-attention module where d is the hidden dimension and $h_i^{(l)} \in \mathbb{R}^{1 \times d}$ is the hidden representation at position i . The input H is projected by three matrices $W_Q^h \in \mathbb{R}^{d \times d_K}$, $W_K^h \in \mathbb{R}^{d \times d_K}$ and $W_V^h \in \mathbb{R}^{d \times d_V}$ to the corresponding representations W_Q^h, W_K^h, W_V^h for each head h . A is a matrix capturing the similarity between queries and keys for each head h and $\|_h$ is concatenation operation. LN is layer normalization and FFN is the feed-forward network. For simplicity, we omit bias terms and assume $d_K = d_V = d$.

C Datasets and Preprocessing

C.1 Real Datasets

For **AIDS(2-15)**, **LINUX(2-15)**, we randomly selected 1500 graphs whose size range from 2 to 15 in the **AIDS** [30] and **LINUX** [39]. For **PTC_MM(all)**, we use the all graphs in the **PTC_MM** [11]. Each dataset is randomly split 80%, 10%, and 10% of all the graphs as original training set, original validation set, and original testing set, respectively. Then, each graph in the original set is paired with another graph as a sample. The datasets statistics for the regression task is shown in Table. 6.

Table 6: Statistics of AIDS, LINUX and PTC_MM. B (Billion), M (Million).

	$\# G $	$Avg.(V , E)$	#Labels	# Graph Pairs
AIDS(2-15)	1500	(10.22, 20.39)	38	225M
LINUX(2-15)	1500	(9.40, 15.58)	1	225M
PTC_MM(all)	336	(13.97, 28.64)	20	~11.2M

For MCS metric, we use MCSPLIT [26] to calculate the MCS for a pair of graphs and then normalize it to similarity score: $nMCS(\mathcal{G}_1, \mathcal{G}_2) = \frac{MCS(\mathcal{G}_1, \mathcal{G}_2)}{(|\mathcal{G}_1| + |\mathcal{G}_2|)/2}$. For GED metric, we use A* [32] to compute GED for graphs. For graphs that can not be computed by A* in 1000 seconds, we take the minimum distance computed by BEAM [27], HUNGARIAN [31], VJ [8] and HED [9], since their returned GEDs are guaranteed to be upper bounds of the true GEDs. Figure. 9 presents the proportion of exact and approximate GED-labels on the three datasets. Next, we normalize it to similarity score: $nGED(\mathcal{G}_1, \mathcal{G}_2) = \exp(\frac{-GED(\mathcal{G}_1, \mathcal{G}_2)}{(|\mathcal{G}_1| + |\mathcal{G}_2|)/2})$. Figure. 10 presents the distribution of the similarity score on two metric.

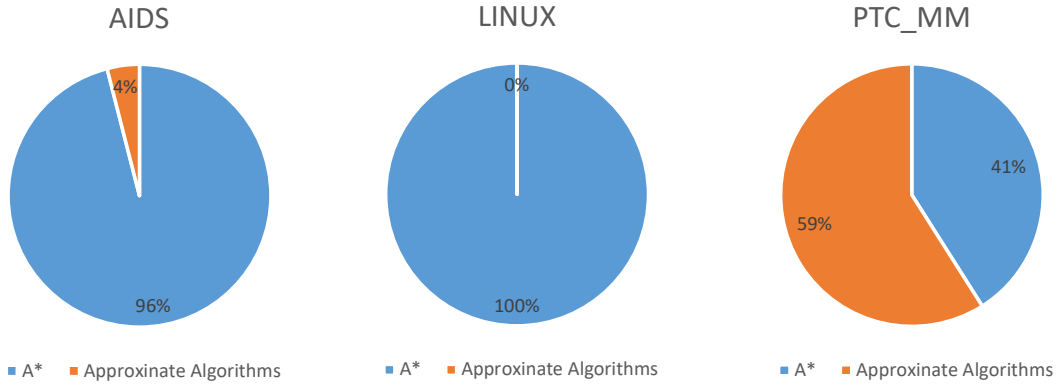


Figure 9: The proportion of exact and approximate GED-labels.

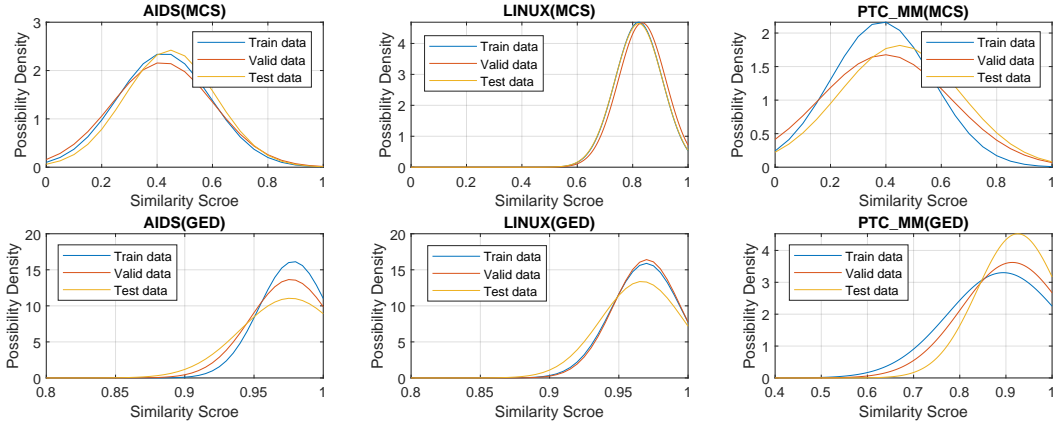


Figure 10: The distribution of the real datasets.

For the classification task, we split **FFmpeg** and **OpenSSL** into 3 sub-datasets (i.e., [3, 200], [20,200], and [50,200]) according to the size ranges of pairs of input graphs. Table. 7 shows the statistics of these datasets.

Table 7: Statistic of FFmpeg and OpenSSL. B (Billion), M (Million).

	Subsets	$\# G $	$Avg. V $	$Avg. E $	# Graph Pairs
FFmpeg	[3, 200]	83008	18.83	27.02	6.89B
	[20, 200]	31696	51.02	75.88	1B
	[50, 200]	10824	90.93	136.83	117M
OpenSSL	[3, 200]	73953	15.73	21.97	5.46B
	[20, 200]	15800	44.89	67.15	249M
	[50, 200]	4308	83.68	127.75	18.5M

C.2 Synthetic Datasets

To verify the performance on large graphs, we also use the Barabási–Albert model [13] to generate synthetic graphs. We generated three sythetic datasets with graph sizes around 100, 200, and 300 respectively, called **BA100**, **BA200** and **BA300**.

MCS metric We randomly generate a core graph by BA-model for each example and take this core as the primary graph. Next, we add edges and nodes to its surroundings randomly, thereby obtaining g_1 and g_2 . We regard the core as the MCS and then obtain the similarity score. For instance, the size of the core graph is 60, and the number of added nodes for g_1 is 35, for g_2 is 45, thus the final label is 0.6. Although the size of the real MCS may be more than 60, it is the lower bound for this sample. The range of core graph size and added nodes are shown in Table 8. The pseudocode is shown in the Alg. 1.

Table 8: Statistics of BA-graph for MCS metric.

	# Size of Core	# Added Nodes	# Train Pairs	# Valid Pairs	# Test Pairs
BA100	(50, 70)	(30, 50)	32000	4000	4000
BA200	(100, 120)	(80, 100)	32000	4000	4000
BA300	(150, 170)	(130, 150)	32000	4000	4000

Algorithm 1: Generate BA graphs for MCS metric

Input: (c_1, c_2) for the range of the number of core graph nodes; (a_1, a_2) for the range of the number of added graph nodes; n for the number of samples

Output: BA datasets in MCS metric

```

1 data  $\leftarrow \{\}$ ;
2 for  $i \leftarrow 0$  to  $n$  do
3    $c \leftarrow \text{random}(c_1, c_2)$ ;
4    $a_1 \leftarrow \text{random}(a_1, a_2)$ ;
5    $a_2 \leftarrow \text{random}(a_1, a_2)$ ;
6   // use BA-model to generate the core graph with  $c$  nodes
    $\text{core} \leftarrow \text{barabasi\_albert\_graph}(c)$ ;
   // use BA-model to generate two graphs based on the core graph, and
   // they have  $c + a$  nodes
7    $g_1^i \leftarrow \text{barabasi\_albert\_graph}(c + a_1, \text{core})$ ;
8    $g_2^i \leftarrow \text{barabasi\_albert\_graph}(c + a_2, \text{core})$ ;
9    $\text{sim} \leftarrow c / (c + 0.5 \times (a_1 + a_2))$ ;
10   $\{g_1^i, g_2^i, \text{sim}\} \parallel \text{data}$ ;
11 end

```

GED metric Firstly, we generated two basic graphs by BA-model. To each of them, it is edited by **1.** Deleting a leaf node and its edge **2.** Adding a leaf node **3.** Adding an edge among existing node. The trimming step n from the basic graph g to the generated one g_i ranges from 1 to 10, which means the GED score between g and g_i ranges from 1 to 10. In order to get more data, we combine two generated graphs and derive the GED by adding their edit distances coming from the basic graph $(n_1 + n_2)$, If the GED computed by BEAM [27], HUNGARIAN [31], VJ [8] and HED [9] is less than $n_1 + n_2$, we use the GED computed by the approximate algorithm. The datasets statistics is shown in Table. 9. The pseudocode is shown in the Alg. 2.

Table 9: Statistics of BA-graph for GED metric.

	# Basic Graph	# Nodes	# Train Pairs	# Valid Pairs	# Test Pairs
BA100	2	100	32000	4000	4000
BA200	2	200	32000	4000	4000
BA300	2	300	32000	4000	4000

Algorithm 2: Generate BA graphs for GED metric

Input: b for the number of basic graph nodes; n for the number of generated samples to store in one collection

Output: BA datasets in GED metric

```

1  $data \leftarrow \{\}$ ;
2  $ged \leftarrow 0$ ;
3  $A \leftarrow \{\}$ ;
4  $B \leftarrow \{\}$ ;
5 Generate two collections of graphs;
6 for  $i \leftarrow 0$  to  $n$  do
    // use BA-model to generate two basic graphs with  $b$  nodes
7      $b_1 \leftarrow \text{barabasi\_albert\_graph}(b)$ ;
8      $b_2 \leftarrow \text{barabasi\_albert\_graph}(b)$ ;
    // every 10 iterations, increase ged
9     if  $i \% 10 = 0$  then
10        |  $ged \leftarrow ged + 1$ ;
11    end
    // the trimming methods are 1.deleting a leaf node and its edge
    // 2.adding a leaf node and 3.adding an edge, which have the same
    // possibility to operate for each time
12     $g_1 \leftarrow \text{trim\_ged\_times}(b_1)$ ;
13     $g_2 \leftarrow \text{trim\_ged\_times}(b_2)$ ;
14     $\{g_1, ged\} || A$ ;
15     $\{g_2, ged\} || B$ ;
16 end
17 Pack and label graphs;
18  $C \leftarrow A || B$ ;
19 for  $i \leftarrow 0$  to  $2n$  do
20     for  $j \leftarrow 0$  to  $2n$  do
21         |  $(g_1, ged_1) \leftarrow C[i]$ ;
22         |  $(g_2, ged_2) \leftarrow C[j]$ ;
23         |  $ged \leftarrow \min(ged_1 + ged_2, \min(\text{BEAM}, \text{HUNGRIAN}, \text{VJ}, \text{HED}))$ ;
24         |  $sim \leftarrow \exp(\frac{-ged}{(|g_1|+|g_2|)/2})$ ;
25         |  $\{g_1, g_2, sim\} || data$ ;
26     end
27 end

```

D The Results for GED Metric

The regression results on the GED metric can be found in Table. 10.

E Hyperparameter Settings

For all datasets, the GCN learning layer is fixed to 3, and the transformer encoder head number is set to 8; The scope of the hyperparameter search is shown in the Table. 12. The results of the hyperparameter search are shown in Table. 13.

Table 10: The regression results for the GED metric ($\text{mse} \times 10^{-2}$).

Metrics	AIDS(2-15)			LINUX(2-15)			PTC_MM(all)		
	mse↓	ρ ↑	p@10↑	mse↓	ρ ↑	p@10↑	mse↓	ρ ↑	p@10↑
GMN	0.19	0.0918	0.1857	0.20	0.0662	0.1400	1.33	0.0117	0.3324
GraphSim	0.09	0.3513	0.0641	0.10	0.1457	0.1400	0.98	0.1714	0.3382
SimGNN	0.07	0.4056	0.1342	0.11	0.4006	0.0810	1.18	0.1451	0.3382
SMPNN	15.61	0.1583	0.0634	21.95	0.0422	0.055	21.27	0.0806	0.3088
MGMN	0.08	0.2905	0.0437	0.08	0.2192	0.0106	1.17	0.1630	0.0891
PSimGNN	0.09	0.3361	0.0534	0.11	0.1803	0.0093	1.21	0.1520	0.0437
H2MN	0.07	0.3988	0.0540	0.07	0.3813	0.2763	0.96	0.1531	0.0990
INFMCS	0.04	0.4090	0.1854	0.04	0.4054	0.3445	0.68	0.1768	0.3406

Table 12: The scope of hyperparameter search.

Parameter	Values
# GCN layer	3
GCN hidden dimension	{128, 256, 512}
# Transformer head	8
# Transformer layer	{2, 4, 6, 8}
Batch size	128 (regression) / 32 (classification)
Learning rate	0.001
# Epoch	100 (regression) / 30 (classification)

F Complexity Analysis

In this section, we analyze the time complexity of our proposed INFMCS. Here, l_1 denotes the number of GCN layers, l_2 denotes the number of Transformer Encoder layers, d represents the hidden dimension and h is number of heads in Transformer. First, the complexity of GCN is $\mathcal{O}(l_1|\mathcal{E}||\mathcal{V}|d^2)$. Second, closeness centrality requires the time of $\mathcal{O}(|\mathcal{V}|\log|\mathcal{V}| + |\mathcal{E}|)$. The complexity of Transformer is $\mathcal{O}(l_2|\mathcal{V}|^2dh)$. Third, the complexity of cross-propagation is $\mathcal{O}(|\mathcal{V}_1||\mathcal{V}_2|)$.

G Comparison with Graphormer

Graphormer [44] is a SOTA graph transformer model on the recent OGB-LSC [12] quantum chemistry regression (i.e., PCQM4M-LSC) challenge, which is currently the biggest graph-level prediction dataset. We also use it in our computation paradigm, and the results are shown in Table 11. To save computational resources and avoid overfitting, we set the number of layers to 5, the hidden dimension to 128, and the number of heads to 8 in Graphormer. We find that GCwT is more suitable for graph similarity computation tasks since Graphormer mainly focuses on the graph-level prediction task.

Table 11: The results of Graphormer. A, L, P denote AIDS, LINUX, PTC_MM.

Datasets	A	L	P	FFmpeg			OpenSSL		
				[3, 2H]	[20, 2H]	[50, 2H]	[3, 2H]	[20, 2H]	[50, 2H]
	mse($\times 10^{-2}$)			AUC score					
Gomer	1.49	0.31	1.15	97.95	98.41	98.03	97.24	98.17	97.74
Ours	0.30	0.02	0.71	98.49	99.36	99.49	98.34	99.14	99.26

H The number of parameters

A comparison of the number of parameters of our method with other baselines can be found in Table 14.

Table 13: The results of hyperparameter search.

		FFmpeg			OpenSSL		
		[3, 200]	[20, 200]	[50, 200]	[3, 200]	[20, 200]	[50, 200]
l		8	6	6	4	8	8
d		256	128	128	256	256	256
MCS metric							
		AIDS	LINUX	PTC_MM	BA100	BA200	BA300
l		2	2	3	3	2	4
d		128	256	128	256	128	128
GED metric							
		AIDS	LINUX	PTC_MM	BA100	BA200	BA300
l		2	2	3	3	2	3
d		128	256	128	128	128	128

Table 14: The number of parameters

Model	EMBAVG	GMN	GraphSim	SimGNN	SMPNN
Number of Parameters	26K	62K	2M	17K	13K
Model	H2MN	GOTSim	Base(ours)	INFMCS(ours)	Graphomer
Number of Parameters	291K	75K	18K	306K	216M

References

- [1] Yunsheng Bai, Hao Ding, Song Bian, Ting Chen, Yizhou Sun, and Wei Wang. Simgnn: A neural network approach to fast graph similarity computation. In *Proceedings of the Twelfth ACM International Conference on Web Search and Data Mining*, pages 384–392, 2019.
- [2] Yunsheng Bai, Hao Ding, Ken Gu, Yizhou Sun, and Wei Wang. Learning-based efficient graph similarity computation via multi-scale convolutional set matching. In *Proceedings of the AAAI Conference on Artificial Intelligence*, volume 34, pages 3219–3226, 2020.
- [3] David B Blumenthal and Johann Gamper. On the exact computation of the graph edit distance. *Pattern Recognition Letters*, 134:46–57, 2020.
- [4] Andrew P Bradley. The use of the area under the roc curve in the evaluation of machine learning algorithms. *Pattern recognition*, 30(7):1145–1159, 1997.
- [5] Horst Bunke. What is the distance between graphs. *Bulletin of the EATCS*, 20:35–39, 1983.
- [6] Horst Bunke and Kim Shearer. A graph distance metric based on the maximal common subgraph. *Pattern recognition letters*, 19(3-4):255–259, 1998.
- [7] Khoa D Doan, Saurav Manchanda, Suchismit Mahapatra, and Chandan K Reddy. Interpretable graph similarity computation via differentiable optimal alignment of node embeddings. In *Proceedings of the 44th International ACM SIGIR Conference on Research and Development in Information Retrieval*, pages 665–674, 2021.
- [8] Stefan Fankhauser, Kaspar Riesen, and Horst Bunke. Speeding up graph edit distance computation through fast bipartite matching. In *International Workshop on Graph-Based Representations in Pattern Recognition*, pages 102–111. Springer, 2011.
- [9] Andreas Fischer, Ching Y Suen, Volkmar Frinken, Kaspar Riesen, and Horst Bunke. Approximation of graph edit distance based on hausdorff matching. *Pattern Recognition*, 48(2):331–343, 2015.
- [10] Reza Ghaeini, Xiaoli Z Fern, and Prasad Tadepalli. Interpreting recurrent and attention-based neural models: a case study on natural language inference. *arXiv preprint arXiv:1808.03894*, 2018.
- [11] Christoph Helma, Ross D. King, Stefan Kramer, and Ashwin Srinivasan. The predictive toxicology challenge 2000–2001. *Bioinformatics*, 17(1):107–108, 2001.

- [12] Weihua Hu, Matthias Fey, Hongyu Ren, Maho Nakata, Yuxiao Dong, and Jure Leskovec. Ogb-lsc: A large-scale challenge for machine learning on graphs. *arXiv preprint arXiv:2103.09430*, 2021.
- [13] Hawoong Jeong, Zoltan Néda, and Albert-László Barabási. Measuring preferential attachment in evolving networks. *EPL (Europhysics Letters)*, 61(4):567, 2003.
- [14] Diederik P Kingma and Jimmy Ba. Adam: A method for stochastic optimization. In *International Conference on Learning Representations*, 2015.
- [15] Thomas N Kipf and Max Welling. Semi-supervised classification with graph convolutional networks. *arXiv preprint arXiv:1609.02907*, 2016.
- [16] Sofia Ira Ktena, Sarah Parisot, Enzo Ferrante, Martin Rajchl, Matthew Lee, Ben Glocker, and Daniel Rueckert. Distance metric learning using graph convolutional networks: Application to functional brain networks. In *International Conference on Medical Image Computing and Computer-Assisted Intervention*, pages 469–477. Springer, 2017.
- [17] Zixun Lan, Ye Ma, Limin Yu, Linglong Yuan, and Fei Ma. Aednet: Adaptive edge-deleting network for subgraph matching. *Pattern Recognition*, page 109033, 2022.
- [18] Zixun Lan, Limin Yu, Linglong Yuan, Zili Wu, Qiang Niu, and Fei Ma. Sub-gmn: The subgraph matching network model. *arXiv preprint arXiv:2104.00186*, 2021.
- [19] Yujia Li, Chenjie Gu, Thomas Dullien, Oriol Vinyals, and Pushmeet Kohli. Graph matching networks for learning the similarity of graph structured objects. In *International conference on machine learning*, pages 3835–3845. PMLR, 2019.
- [20] Zhouhan Lin, Minwei Feng, Cicero Nogueira dos Santos, Mo Yu, Bing Xiang, Bowen Zhou, and Yoshua Bengio. A structured self-attentive sentence embedding. *arXiv preprint arXiv:1703.03130*, 2017.
- [21] Xiang Ling, Lingfei Wu, Saizhuo Wang, Tengfei Ma, Fangli Xu, Alex X Liu, Chunming Wu, and Shouling Ji. Multilevel graph matching networks for deep graph similarity learning. *IEEE Transactions on Neural Networks and Learning Systems*, 2021.
- [22] Yang Liu and Mirella Lapata. Learning structured text representations. *Transactions of the Association for Computational Linguistics*, 6:63–75, 2018.
- [23] Minh-Thang Luong, Hieu Pham, and Christopher D Manning. Effective approaches to attention-based neural machine translation. *arXiv preprint arXiv:1508.04025*, 2015.
- [24] Guixiang Ma, Nesreen K Ahmed, Theodore L Willke, Dipanjan Sengupta, Michael W Cole, Nicholas B Turk-Browne, and Philip S Yu. Deep graph similarity learning for brain data analysis. In *Proceedings of the 28th ACM International Conference on Information and Knowledge Management*, pages 2743–2751, 2019.
- [25] Ye Ma, Zixun Lan, Lu Zong, and Kaizhu Huang. Global-aware beam search for neural abstractive summarization. *Advances in Neural Information Processing Systems*, 34, 2021.
- [26] Ciaran McCreesh, Patrick Prosser, and James Trimble. A partitioning algorithm for maximum common subgraph problems. In *IJCAI*, 2017.
- [27] Michel Neuhaus, Kaspar Riesen, and Horst Bunke. Fast suboptimal algorithms for the computation of graph edit distance. In *Joint IAPR International Workshops on Statistical Techniques in Pattern Recognition (SPR) and Structural and Syntactic Pattern Recognition (SSPR)*, pages 163–172. Springer, 2006.
- [28] Adam Paszke, Sam Gross, Francisco Massa, Adam Lerer, James Bradbury, Gregory Chanan, Trevor Killeen, Zeming Lin, Natalia Gimelshein, Luca Antiga, et al. Pytorch: An imperative style, high-performance deep learning library. *Advances in neural information processing systems*, 32, 2019.

- [29] Pau Riba, Andreas Fischer, Josep Lladós, and Alicia Fornés. Learning graph distances with message passing neural networks. In *2018 24th International Conference on Pattern Recognition (ICPR)*, pages 2239–2244. IEEE, 2018.
- [30] Kaspar Riesen and Horst Bunke. Iam graph database repository for graph based pattern recognition and machine learning. In *Joint IAPR International Workshops on Statistical Techniques in Pattern Recognition (SPR) and Structural and Syntactic Pattern Recognition (SSPR)*, pages 287–297. Springer, 2008.
- [31] Kaspar Riesen and Horst Bunke. Approximate graph edit distance computation by means of bipartite graph matching. *Image and Vision computing*, 27(7):950–959, 2009.
- [32] Kaspar Riesen, Sandro Emmenegger, and Horst Bunke. A novel software toolkit for graph edit distance computation. In *International Workshop on Graph-Based Representations in Pattern Recognition*, pages 142–151. Springer, 2013.
- [33] Yu Rong, Wenbing Huang, Tingyang Xu, and Junzhou Huang. Dropedge: Towards deep graph convolutional networks on node classification. *arXiv preprint arXiv:1907.10903*, 2019.
- [34] Charles Spearman. The proof and measurement of association between two things. 1961.
- [35] Shikhar Vashishth, Shyam Upadhyay, Gaurav Singh Tomar, and Manaal Faruqui. Attention interpretability across nlp tasks. *arXiv preprint arXiv:1909.11218*, 2019.
- [36] Ashish Vaswani, Noam Shazeer, Niki Parmar, Jakob Uszkoreit, Llion Jones, Aidan N Gomez, Łukasz Kaiser, and Illia Polosukhin. Attention is all you need. *Advances in neural information processing systems*, 30, 2017.
- [37] Minjie Wang, Da Zheng, Zihao Ye, Quan Gan, Mufei Li, Xiang Song, Jinjing Zhou, Chao Ma, Lingfan Yu, Yu Gai, Tianjun Xiao, Tong He, George Karypis, Jinyang Li, and Zheng Zhang. Deep graph library: A graph-centric, highly-performant package for graph neural networks. *arXiv preprint arXiv:1909.01315*, 2019.
- [38] Shen Wang, Zhengzhang Chen, Xiao Yu, Ding Li, Jingchao Ni, Lu-An Tang, Jiaping Gui, Zhichun Li, Haifeng Chen, and Philip S Yu. Heterogeneous graph matching networks. *arXiv preprint arXiv:1910.08074*, 2019.
- [39] Xiaoli Wang, Xiaofeng Ding, Anthony KH Tung, Shanshan Ying, and Hai Jin. An efficient graph indexing method. In *2012 IEEE 28th International Conference on Data Engineering*, pages 210–221. IEEE, 2012.
- [40] Yequan Wang, Minlie Huang, Xiaoyan Zhu, and Li Zhao. Attention-based lstm for aspect-level sentiment classification. In *Proceedings of the 2016 conference on empirical methods in natural language processing*, pages 606–615, 2016.
- [41] Stanley Wasserman, Katherine Faust, et al. *Social network analysis: Methods and applications*. 1994.
- [42] Haoyan Xu, Ziheng Duan, Yueyang Wang, Jie Feng, Runjian Chen, Qianru Zhang, and Zhongbin Xu. Graph partitioning and graph neural network based hierarchical graph matching for graph similarity computation. *Neurocomputing*, 439:348–362, 2021.
- [43] Xifeng Yan and Jiawei Han. gspan: Graph-based substructure pattern mining. In *2002 IEEE International Conference on Data Mining, 2002. Proceedings.*, pages 721–724. IEEE, 2002.
- [44] Chengxuan Ying, Tianle Cai, Shengjie Luo, Shuxin Zheng, Guolin Ke, Di He, Yanming Shen, and Tie-Yan Liu. Do transformers really perform badly for graph representation? *Advances in Neural Information Processing Systems*, 34, 2021.
- [45] Zhiping Zeng, Anthony KH Tung, Jianyong Wang, Jianhua Feng, and Lizhu Zhou. Comparing stars: On approximating graph edit distance. *Proceedings of the VLDB Endowment*, 2(1):25–36, 2009.
- [46] Zhen Zhang, Jiajun Bu, Martin Ester, Zhao Li, Chengwei Yao, Zhi Yu, and Can Wang. H2mn: Graph similarity learning with hierarchical hypergraph matching networks. In *Proceedings of the 27th ACM SIGKDD Conference on Knowledge Discovery & Data Mining*, pages 2274–2284, 2021.